Nano Energy 36 (2017) 241–249

Contents lists available at ScienceDirect

Nano Energy

journal homepage: www.elsevier.com/locate/nanoen

Full paper

A self-powered sterilization system with both instant and sustainable antibacterial ability

Jingjing Tian[a,b,c,1], Hongqing Feng[a,b,1], Ling Yan[d,1], Min Yu[a,b], Han Ouyang[a,b,c], Hu Li[d], Wen Jiang[a,b,c], Yiming Jin[a,b,c], Guang Zhu[a,b], Zhou Li[a,b,*], Zhong Lin Wang[a,b,e]

[a] Beijing Institute of Nanoenergy and Nanosystems, Chinese Academy of Sciences, Beijing 100083, PR China
[b] CAS Center for Excellence in Nanoscience, National Center for Nanoscience and Technology (NCNST), Beijing 100190, PR China
[c] University of Chinese Academy of Sciences, Beijing 100049, PR China
[d] School of Biological Science and Medical Engineering, Beihang University, Beijing 100191, PR China
[e] School of Materials Science and Engineering, Georgia Institute of Technology, Atlanta, GA 30332-0245, United States

ARTICLE INFO

Keywords:
Triboelectric nanogenerator
Water sterilization
Electroporation
Reactive oxygen species
Electron storage

ABSTRACT

A self-powered and high-efficient water sterilization system was set up consisting of a wave-driven triboelectric nanogenerator (TENG) and two nanobrush electrodes made of Ag-nanoparticles integrated ZnO-nanowires. The system showed both instant and sustainable sterilization efficiency for various microbes including those in natural river water. The colony forming units (CFU) were reduced from 10^6/mL to 0 within 0.5 min of electrical field (EF) treatment for Gram-negative bacteria. In addition, the bacteria annihilation ability was sustained for at least 20 min after withdrawing the EF. The mechanism lay in the synergetic work of electricity and the Ag/ZnO nanomaterial, which not only produced electroporation during EF treatment, but also induced sustained intracellular reactive oxygen species (ROS) to do additional sterilization when EF was withdrawn.

1. Introduction

One of the critical problems affecting people's quality of life is lack of clean water, especially in developing areas. Water contaminated by pathogens may lead to infectious epidemic diseases such as diarrhea [1,2]. The existing chemical and physical water sterilization methods both have critical drawbacks. Chemical methods including chlorination, ozone or other oxidizing agent may form carcinogenic by-products and raise health concerns [3,4]. Physical methods such as membrane filtration, ultrasonic wave and ultraviolet have limited handling capacity and high energy consumption [5,6]. As a result, new robust water disinfection methods with non-harmful by-products, low-cost and high handling capacity are still greatly desired.

Pulsed high electric field (PHEF) sterilization, which has been widely used in rapid disinfection of food and milk, is an attractive candidate for water sterilization due to its short treatment time and no by-products [7,8]. When the PHEF exceeds a certain critical voltage, the cell electroporation and the membranes disruption will occur in living cells including bacteria [9–11]. However, the energy cost for PHEF generation is very high, which largely limits its wide application. Irreversible electroporation caused by PHEF often requires the electrical field (EF) to be larger than 10^6 V/m [12,13]. To reduce the dependence on the high voltage, nanomaterials are introduced. Conductive nanostructure electrodes can generate EF larger than 10^6 V/m at the surrounding area at voltages of less than 100 V [14–16]. However, external electricity supply is still required to carry out the electroporation sterilization.

Recently, triboelectric nanogenerators (TENG) have attracted much attention because it can convert ambient mechanical energy into electricity and become self-powered [17,18]. The working mechanism of the TENG is based on the combination of contact electrification and electrostatic induction. Successfully developed TENG can drive hundreds of light emitting diodes (LED) [19], charge a lithium-ion battery [20,21], or collect energy from muscle motion *in vivo* and *in vitro* for medical applications [22–25]. Also, TENG directly collecting energy from water waves have been reported [26–32].

In this work, a self-powered water sterilization system was developed, which was comprised of a ball-in-ball TENG and Ag nanoparticles (Ag-NP) integrated ZnO nanowires (ZnO-NW) nanobrush electrodes. This self-powered water sterilization system showed both instant and sustainable high-efficient sterilization effect on *Escherichia coli* (*E.coli*), *Staphylococcus aureus* (*S.aureus*) and the natural living bacteria in raw river water. The colony forming units (CFU) of *E. coli* were reduced from

* Corresponding author at: Beijing Institute of Nanoenergy and Nanosystems, Chinese Academy of Sciences, Beijing 100083, PR China.
E-mail address: zli@binn.cas.cn (Z. Li).
[1] J.J. Tian, H.Q. Feng, and L. Yan contributed equally to this work.

http://dx.doi.org/10.1016/j.nanoen.2017.04.030
Received 23 February 2017; Received in revised form 6 April 2017; Accepted 16 April 2017
Available online 23 April 2017

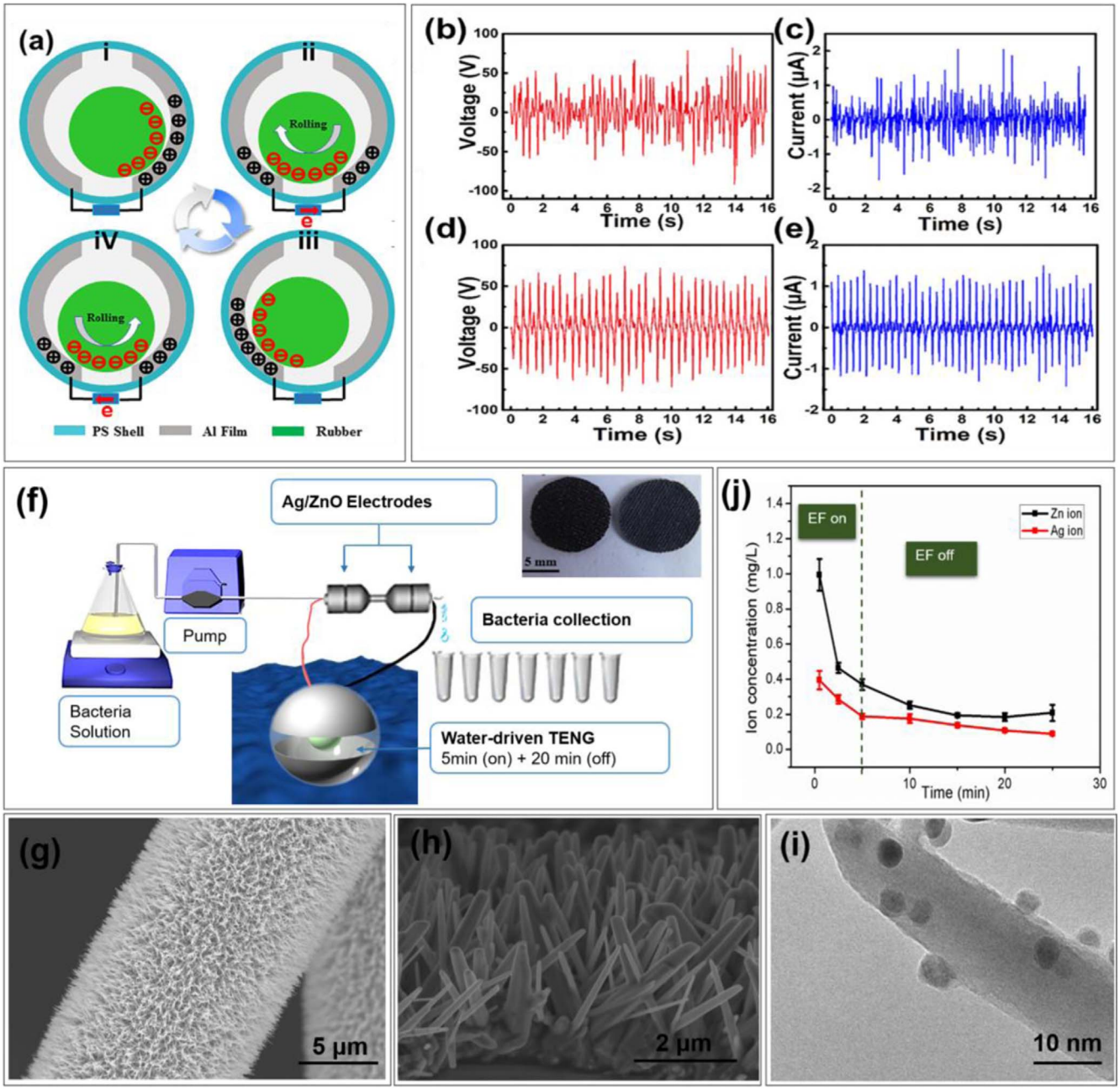

Fig. 1. (a) The design and working mode of the wave-driven TENG. (b, c) The open-circuit voltage and the short-circuit current of the TENG driven by water waves. (d, e) Similar output can be achieved by hand-shaking of the TENG. (f) Schematic diagram of the experimental setup with the TENG and Ag/ZnO electrodes sterilization system; the inset was CC before (left) and after (right) the growth of Ag/ZnO nanobrush; (g, h) SEM pictures showing ZnO-NW grow perpendicularly onto the CC fibers; (i) TEM image showing the Ag-NP tightly attached to ZnO-NW without aggregation. (j) The concentration of the released Zn and Ag ions in the 25 min (n=3).

10^6/mL to 0 within 0.5 min treatment. The annihilation ability was sustained for at least 20 min after the EF supplied by TENG was withdrawn. Strong and long-term reactive oxygen species (ROS) were detected in the bacteria cells, which played the role of water sterilization after the EF was withdrawn. The EF supplied by the TENG, the size effect of Ag/ZnO nanobrush and their electron-storage properties worked synergistically to achieve this high and sustainable sterilization effect.

2. Results and discussions

The TENG in our sterilization system was built with a ball-in-ball structure, and the triboelectric layers were rubber and aluminum (Al) foil (Fig. 1(a)). Four typical states represented its working cycle: at the beginning, the rubber ball stayed at the bottom of the PS shell and adhered to one of the Al foil. Due to triboelectric effect, equal amount of positive and negative charges were formed on the surface of Al foil and rubber ball respectively, which reached an electrostatic equilibrium state (Fig. 1(a i)). When the rubber ball started rolling due to waves and separated from the initial Al foil, the equilibrium state was broken, electrons flowed from the other piece of Al foil through external circuit (Fig. 1(a ii)) until a new equilibrium state was created when the rubber completely adhered onto the latter Al foil (Fig. 1(a iii)). Then the rubber ball started to roll back to the initial Al foil and the electrons began to flow in an opposite direction in the external circuit (Fig. 1(aiv)). The wave-driven TENG output an open-circuit voltage of 50 V and a short-circuit current of about 2 μA (Fig. 1(b), (c)). A similar output was obtained by simply hand shaking of the TENG ball (Fig. 1(d), (e)).

The sterilization experiment setup was shown in Fig. 1(f). The

electricity generated by the TENG was applied on two carbon cloth (CC) electrodes with Ag/ZnO nanobrush growing on the fibers. The Ag/ZnO electrodes were fixed in two filter holders. The bacteria solution passed through them at a constant speed of 1 mL/min driven by a peristaltic pump, and was collected dropwise. The TENG was driven for only 5 min in this experiment. After 5 min, the TENG was stopped from working and providing EF to the electrodes, while the bacteria solutions flowed through them for an additional 20 min to evaluate the sterilization efficiency.

The ZnO-NW grew perpendicular to the CC (Fig. 1(g), (h)). The lengths of the ZnO-NW were about 3.5 μm, and the diameters were in a range from 10 to 40 nm. The Ag-NP uniformly adhered on the ZnO-NW without aggregation, and their diameters were 5.13 ± 1.26 nm (Fig. 1(i), n=10). The amount of ZnO and Ag loaded onto the CC (15.79 ± 0.23 mg) were 8.01 ± 1.63 mg and 0.058 ± 0.014 mg, respectively (Fig. S1, n=10). The released Zn and Ag ions in 25 min were shown in Fig. 1(j) (n=3). The trends of both Ag and Zn ions concentration were very similar. They were highest at the beginning, then dropped quickly to a platform. The highest Zn ion concentration was about 1.0 mg/L at 0.5 min, then it dropped to less than 0.4 mg/L after 5 min. Also, the highest Ag ion concentration was about 0.4 mg/L at 0.5 min, then it dropped to about 0.2 mg/L after 5 min. The release was very constant, as tested in 10 cycles of 25 min (Fig. S2). The concentrations of both ions were very low. Even the highest amount of Zn ion was lower than the WHO drink water standard, which was 3 mg/L. Besides, Ag ion concentration of less than 0.5 mg/L didn't have any bacterial inhibition effect as reported in former literature [33]. Hence the low ion release in our system brought in no harmful by-products, and was not the primary reason of sterilization.

The sterilization efficiency of the TENG and Ag/ZnO electrodes system was shown in Fig. 2. The actual CFU numbers were shown in Fig. 2(a) and (b), and the sterilization rate (SR) were shown in Fig. 2 (c) and (d). The sterilization efficiency was extremely high for *E. coli* (Fig. 2 (a) and (c)). The number of *E. coli* CFU dropped from 10^6/mL to 0 within 0.5 min after the EF supply (SR=100%). After EF was withdrawn at 5 min, the anti-bacterial ability was sustained. In the following 20 min, the CFU remained 0 (SR=100%). Meanwhile, the ZnO-NW without Ag-NP also had certain anti-bacterial ability under EF application. The CFU reduced to about 5×10^4/mL in the 5 min electricity treatment. After EF withdrawal, the CFU reduction was also sustained in the following 20 min (SR≈95%). In the groups of original CC with EF (CC+EF), or Ag/ZnO nanobrush without EF, the sterilization efficiency was limited, the CFU were still above 10^6/mL (SR≈50%). These results suggested that EF or Ag/ZnO alone didn't have significant anti-bacterial ability, but the synergetic effects of them produced much higher sterilization. In addition, the sustained anti-bacterial effect of the Ag/ZnO nanobrush after EF had its foundation in ZnO-NW, but was much enhanced by the Ag-NP. With regard to the Gram-positive *S. aureus* (Fig. 2(b) and (d)), the sterilization efficiency was lower than *E. coli*. Ag/ZnO nanobrush with EF resulted in more than two order of magnitude CFU reduction in the 5 min EF treatment (SR≈99%). After EF was withdrawn, the CFU in the afterwards solutions were kept at about 5×10^4/mL in the following 20 min (SR≈95%). ZnO-NW with EF produced lower sterilization effect, similar with the CC with EF, and Ag/ZnO without EF groups (SR≈50%). This difference could be ascribed to the thicker layer of peptidoglycan in the Gram-positive bacteria cell wall than the Gram-negative ones. The peptidoglycan layer performed most of the resistance to external stress, so the Gram-positive *S. aureus* were more difficult to sterilize than Gram-negative *E. coli* [34].

The sterilization ability of our system on natural river water was also tested. Raw river water under Jimen Bridge in Beijing was collected, and flowed through the Ag/ZnO electrodes directly at the same parameters as the *E. coli* and *S. aureus* solutions. The river water was used directly and immediately after obtained from the river to flow through the Ag/ZnO electrodes at a speed of 1 mL/min, and was collected at each time points. 100 μL of the collected water was spread on the LB agar plates, and cultured at 37 °C for 18 h to allow single bacteria grow into visible colony. The collected water was also 10-fold diluted and spread on the LB agar plates to get the best dilution for CFU counting. In Fig. 2(e), the top row were control groups without treatment and the bottom row were treated groups (all without dilution). It was obvious that there were hardly any cultivatable microorganisms in the river water after treatment. The CFU and SR data was shown in Fig. 2(f) and (g). During the 5 min EF treatment, the SR was about 99%, 20 min after EF terminated, the SR was still over 80%.

SEM was employed to study the morphology changes in the bacteria after treatment. Fig. 3(a) and (b) showed the residual bacteria on the CC fibers and Ag/ZnO nanobrush after EF treatment respectively. Only a few bacteria were left on the fibers, and most of them had flowed away with the solution. Pores in the membrane were found in large numbers of *E.coli* bacteria in the flowing out solution (dashed circles in Fig. 3(c)). Similarly, in the treated sample of *S. aureus*, cell membrane damages including pores and fragments aggregation were found (Fig. 3(d)). These results demonstrated that bacteria electroporation had been induced in our system. For the Gram-negative *E.coli*, another morphological change, bacteria filamentation, was found both on the Ag/ZnO nanobrush (Fig. 3(e)) and in the solution (Fig. 3(f)). Bacteria filamentation was often observed as a result of bacteria response to various stresses, including oxidative stress and DNA damage [35]. Thus the filamentation in *E.coli* suggested a possible sterilization contribution from the oxidative stress.

To find out the role of oxidative stress in the sterilization process, we examined the intracellular reactive oxygen species (ROS) in the bacteria cells. The ROS fluorescence intensity in the bacteria cells after treatment was measured by flow-cytometer, and the percentage of ROS positive cells were obtained (Fig. 4(a)). The overall data were illustrated in Fig. 4(b) and (c). For *E. coli* (Fig. 4(b)), contact with ZnO-NW without EF quickly produced about 15% ROS positive cells in the bacteria (0.5 min), but this soon diminished to control level (about 5%). When ZnO-NW were accompanied by EF, there were about 30% ROS positive cells during the 5 min EF treatment, and about 20% in the following 20 min. When contact with Ag/ZnO nanobrush without EF, the ROS positive cell percentage was around 50% during the 25 min treatment. For the Ag/ZnO+EF group, there were about 30% ROS positive cells during the 5 min EF treatment, which was relatively lower. This was because bacteria cells had been mostly disinfected and couldn't be stained by the ROS indicator. In later time points, the ROS positive cells increased to as high as 76.4% at 25 min. For *S. aureus* (Fig. 4c), the sterilization was less effective than *E. coli*, and the ROS signals were also much weaker. For the Ag/ZnO +EF group, the percentage of ROS positive bacteria was raised to 25.4% at 5 min, which was the highest among all the *S. aureus* groups. After the EF was withdrawn, it also showed sustained ROS signals (about 15%). The other groups were almost as low as the control group. The ROS evolution in the two bacteria was highly related to their respective sterilization efficiency. More importantly, ROS was still detected after the 5 min EF treatment, especially in the Ag/ZnO +EF groups. Therefore the intracellular ROS was considered to be the actual reason for the sustainable anti-bacterial ability. The ROS by itself could lead to bacteria cell lysis and death, by interacting with intracellular proteins and inducing proteins denaturation, DNA condensation or respiratory chain disturbance [36,37].

After that, we further explored how the intracellular ROS were continuously induced after the EF was withdrawn. It had been reported that ZnO had electron storage capacity [38,39]. Meanwhile, Ag-NPs would be endowed with strong electron storage ability when combined with semiconductors [40,41]. However, those previous studies were based on Ag-NP incorporated TiO_2 semiconductor under UV excitation. To find out whether that electrons storage priority also existed with our system of EF treatment, the electrons storage performance were characterized by Cyclic Voltammetry (CV) and galvanostatic charge-discharge (CD) in 1 M KNO_3 electrolyte solution. As shown in Fig. 4(d), the absolute area within the CV curve of Ag/ZnO nanobrush was larger than that of ZnO-NW, which suggested a larger capacitance

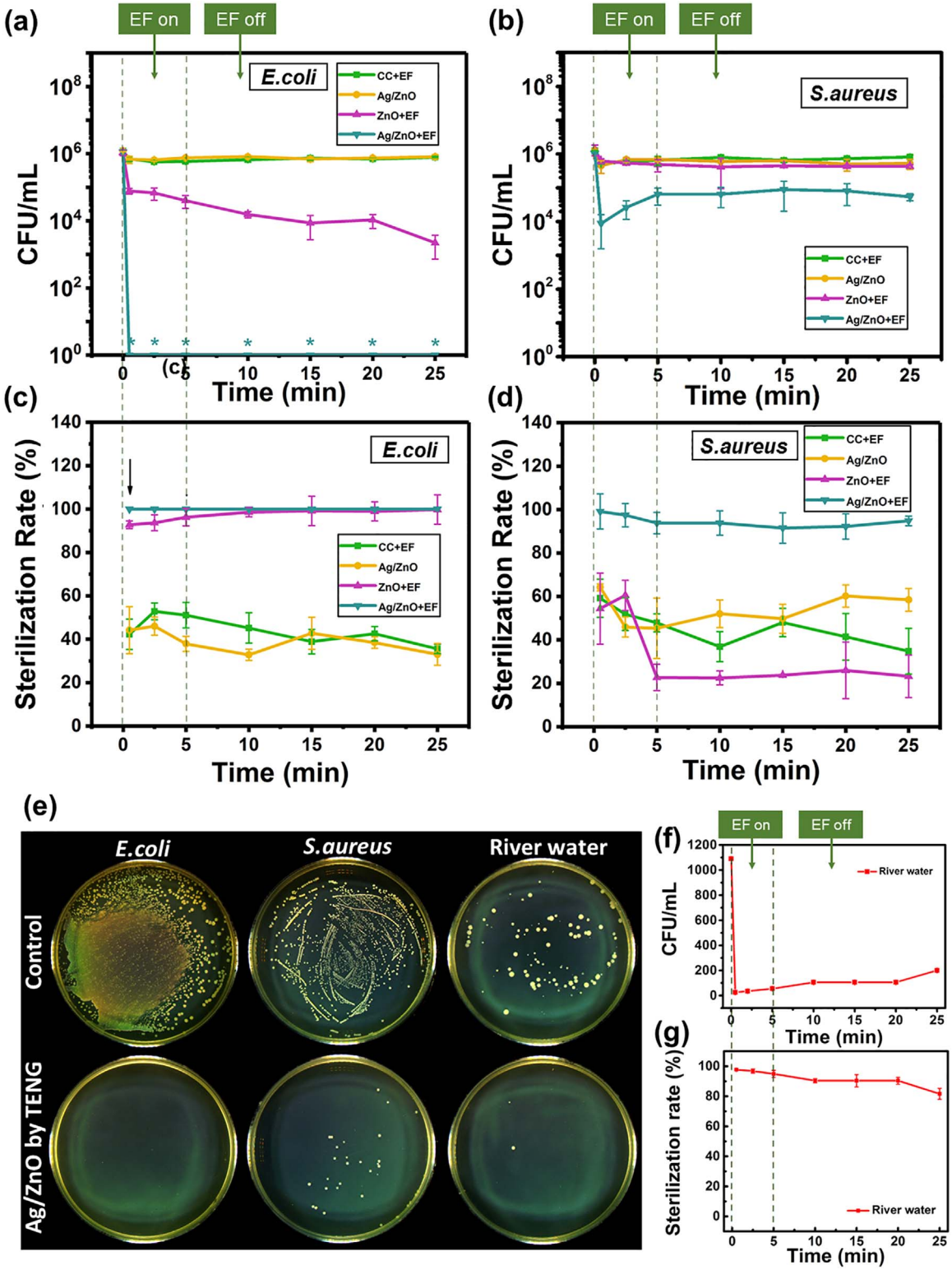

Fig. 2. The sterilization results of the TENG and Ag/ZnO system on *E. coli* (a, c) and *S. aureus* (b, d). (*: CFU=0). (e) The sterilization of mixed bacteria population in natural river water in comparison with *E.coli* and *S.aureus*; the CFU reduced significantly after treatment. (f, g) The CFU and SR of the microbes in the river water.

of Ag/ZnO nanobrush than bulk ZnO. In Fig. 4(e), the discharge time of Ag/ZnO nanobrush was longer than that of ZnO-NW, which also meant a better charge storage capacity of Ag/ZnO nanobrush. On the contrary, in Fig. 4(f), the voltage of carbon fiber arrived only 0.012 V at 5×10^{-8} A, which indicated an inferior charge storage capacity. Because these results were based on one single fiber, the difference would be greatly enlarged in the actual electrodes which consisted of a bunch of fibers. This electron storage property and priority was the reason for the sustainable ROS production. During EF application, large amount of electrons were first stored in Ag-NP, and then in ZnO-NW. After EF withdrawal, the electrons were released to induce ROS production (Eqs. (1) and (2)) [42].

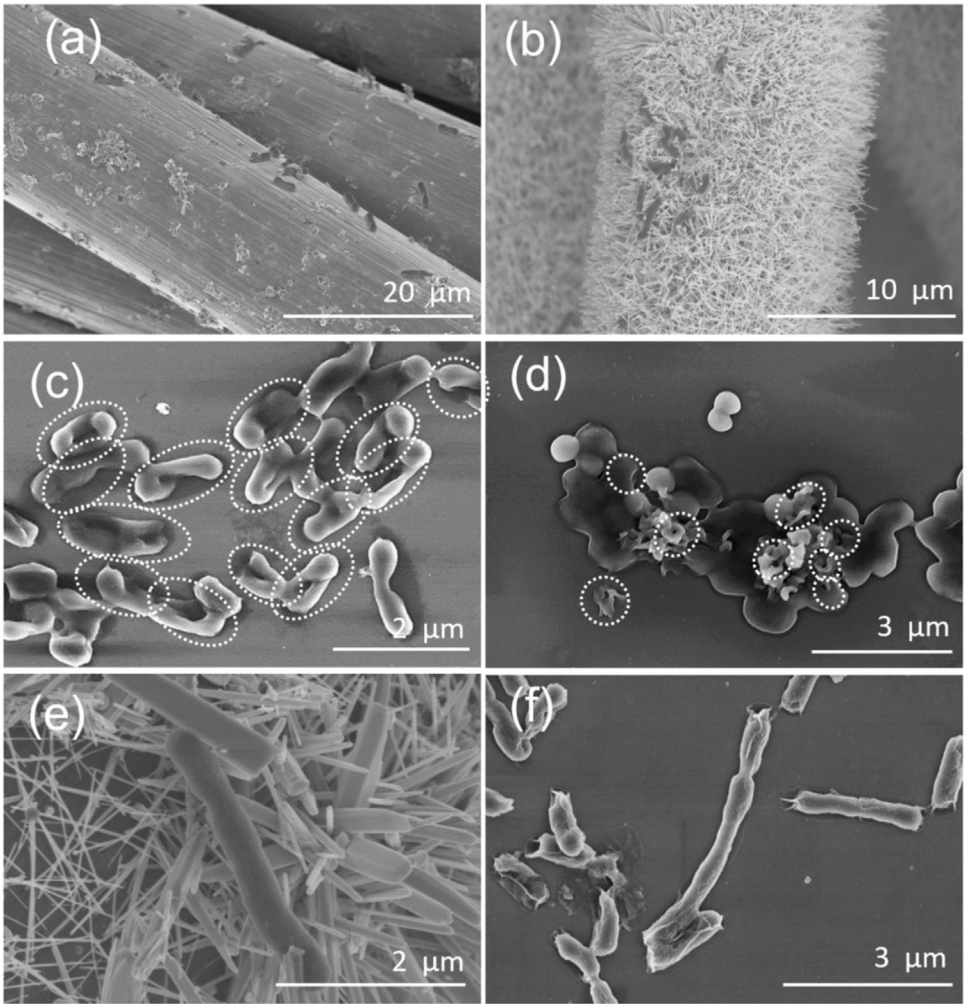

Fig. 3. SEM images of the bacteria after treatment. (a, b) Only a few E. coli cells were left on CC fibers or Ag/ZnO nanobrush after EF treatment. (c) *E. coli* cells in the solution after EF application showed large pores in the membrane (dashed circles). (d) *S. aureus* cells after EF treatment showed pores and structure destructions in the membrane (dashed circles). (e) *E. coli* cells kept on the Ag/ZnO nanobrush after EF treatment showed bacteria filamentation. (f) *E. coli* cells in the solution after EF treatment showed bacteria filamentation.

$$e+O_2 \rightarrow O_2^- \quad (1)$$

$$2H^+ + O_2^- + e \rightarrow H_2O_2 \quad (2)$$

The mechanisms of the instant and sustained anti-bacterial property of our system were illustrated in Fig. 5. During the wave driving time (Fig. 5(a)), TENG not only provided EF between the nanobrush (Fig. 5(b)), but also charged the ZnO-NW or Ag/ZnO nanobrush (Fig. 5(c)). The instant sterilization was ascribed to the electroporation conducted by the NW nanostructure with EF supplied by TENG. The simulation by the finite element method (FEM) showed the EF at the vicinity of the Ag/ZnO nanobrush was above 10^7 V/m at the 50 V voltage provided by the TENG (Fig. 5(b)), which was high enough to induce electroporation. Electroporation resulted in pores and ruptures in bacteria membrane, which directly lead to bacteria death. Furthermore, after waves and EF supply were withdrawn, the stored electrons in Ag/ZnO nanobrush were released slowly. This promoted intracellular ROS production in the flowing through bacteria cells, which continuously sterilized the bacteria. Because the electron storage ability of the Ag/ZnO nanobrush was much larger than the ZnO-NW, the sustainable sterilization ability of the Ag/ZnO+EF group was much more efficient than the ZnO+EF group (Fig. 5(d)).

In this study, we clarified an interesting phenomenon of sustainable sterilization ability of Ag/ZnO electrodes after EF was withdrawn, and the effective time duration was as long as 20 min after 5 min EF application. In addition, the mechanisms were explored and discussed. It was due to the production of intracellular ROS, which was dependent on the electrons storage and release of Ag/ZnO nanobrush after EF treatment. Although sustainable sterilization had been mentioned in Liu's work [43], the effective time duration was only a few minutes, and no explanation to the phenomenon were given in their work. Also, the materials they used was CuO. Excessive Cu ions could be harmful and accumulate in plants and animals [44,45]. On the contrary, Zinc was considered a major trace element for the correct functioning of an organism, playing an important role in maintaining the metabolic homeostasis [46]. Therefore, ZnO could be an advantaged alternative to CuO.

To make clear the role of ROS in the sterilization process, we carried out sensitive and accurate intracellular flow-cytometer ROS assay to detect the oxidative stress induced by our system. Oxidative stress is an important element in many effective anti-bacterial approaches including photocatalysis, radiation, cold plasma, antibiotics, and nanoparticles [47–50]. We succeeded in detecting various ROS intensity in various groups. Also, the induction of intracellular ROS in our system was found to be very quick, because the ROS signal became detectable within 0.5 min after EF treatment. This quick response was comparable to the cold plasma induced oxidative stress in microbes [51]. In fact, the intracellular ROS production is a very complicated process [49,52,53]. The ROS staining in this work demonstrated an increased endogenous oxidative level induced by the electrons released from the electrodes. The ROS could either come from the intracellular oxygen or other molecular that had been excited by the electrons, or from the respiration chain that had been disturbed by the electrons. Respiration was a universal behavior in bacteria that involved

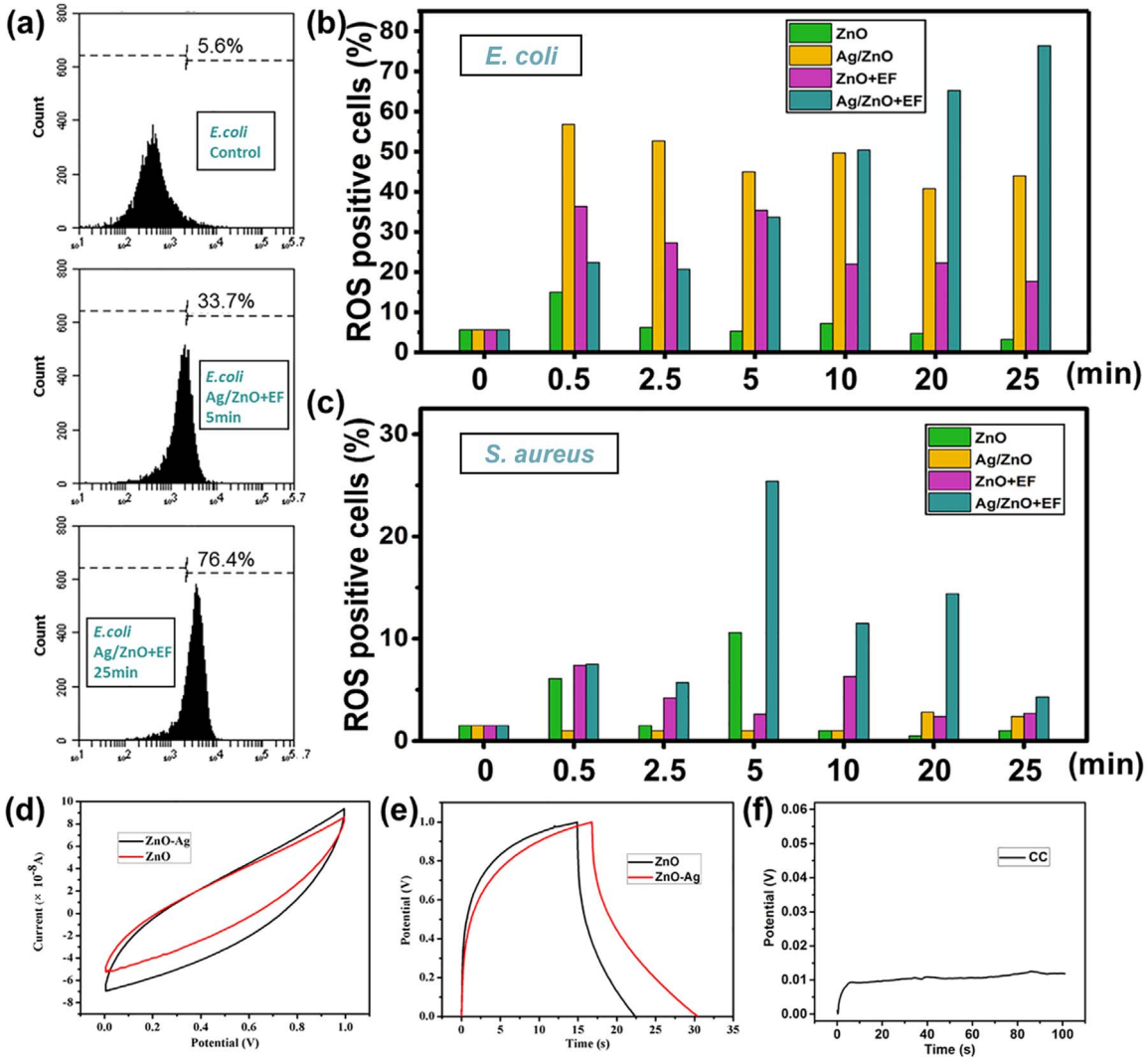

Fig. 4. (a) The intracellular ROS production in bacteria cells was quantitatively measured using flow-cytometer. The percentage of ROS positive cells was obtained based on a uniform ROS intensity threshold set according to the control group. (b, c) The percentage of ROS positive cells of *E. coli* and *S. aureus* were summarized. (d-f) The capacitive performance of a single fiber of ZnO/Ag nanobrush, ZnO-NW and CC, respectively. (d, e) The CV and CD measurement of ZnO/Ag nanobrush and ZnO-NW; (f) The CD measurement of CC.

electron transport [54]. Electrons produced by oxidation of compounds for energy production were finally accepted by O_2 to make H_2O. This process was finished in sequential steps in which ROS was generated and well controlled [55]. But external electrons may disturb the respiration process, result in ROS burst and bacteria death [56]. The exact details of the ROS production in our system were worthy of further exploration.

Our experiment was a small scale study, which revealed in details the sterilization efficiency and mechanism of the combination of TENG and Ag/ZnO nanobrush. In future, electrodes with larger area could be developed to accommodate with larger scale water application. Also, the ball shaped TENG could be integrated into arrays to provide larger output. In natural water, waves occur occasionally, thus the sustainable sterilization ability is a great advantage, because it can continuously sterilize the bacteria even if the electricity generation stops from time to time.

3. Conclusions

An effective water sterilization system was developed consisting of a wave-driven TENG and Ag/ZnO nanobrush electrodes. The sterilization was highly efficient for various organisms including the natural microbes in river water when applying waves on TENG to generate EF. In addition, it also had sustainable bacteria disinfection ability after EF withdrawal. The mechanisms were revealed as follows. First, the Ag/ZnO nanobrush with their nanostructures conducted electroporation in the bacteria at a low voltage produced by the wave-driven TENG. In addition, the Ag-NP incorporated ZnO-NW stored large numbers of electrons when EF was on, and released the electrons when EF was withdrawn, which induced ROS accumulation in the bacteria and sterilized them continuously. Therefore, the wave-driven TENG and Ag/ZnO nanobrush worked synergistically to do water sterilization both instantly and sustainably. This system provided a promising solution for practical natural water sterilization.

4. Experimental section

4.1. Wave driven TENG

The working principle of TENG was previously reported [57]. Our wave-driven TENG was a ball-in-ball design, consisting of a rubber ball (φ=4 cm) rolling freely in a polystyrene (PS) shell (φ=8 cm). Al film were anchored to the inside of the PS shell and functioned as the triboelectric layers and electrodes. The Al film and rubber ball surface were polished with sandpaper (600 mesh) and cleaned with oxygen plasma for 5 min to increase the roughness and voltage output. Then the PS shell was encapsuled with polydimethylsiloxane (PDMS) to avoid water leaking into the triboelectric layers. Electricity was

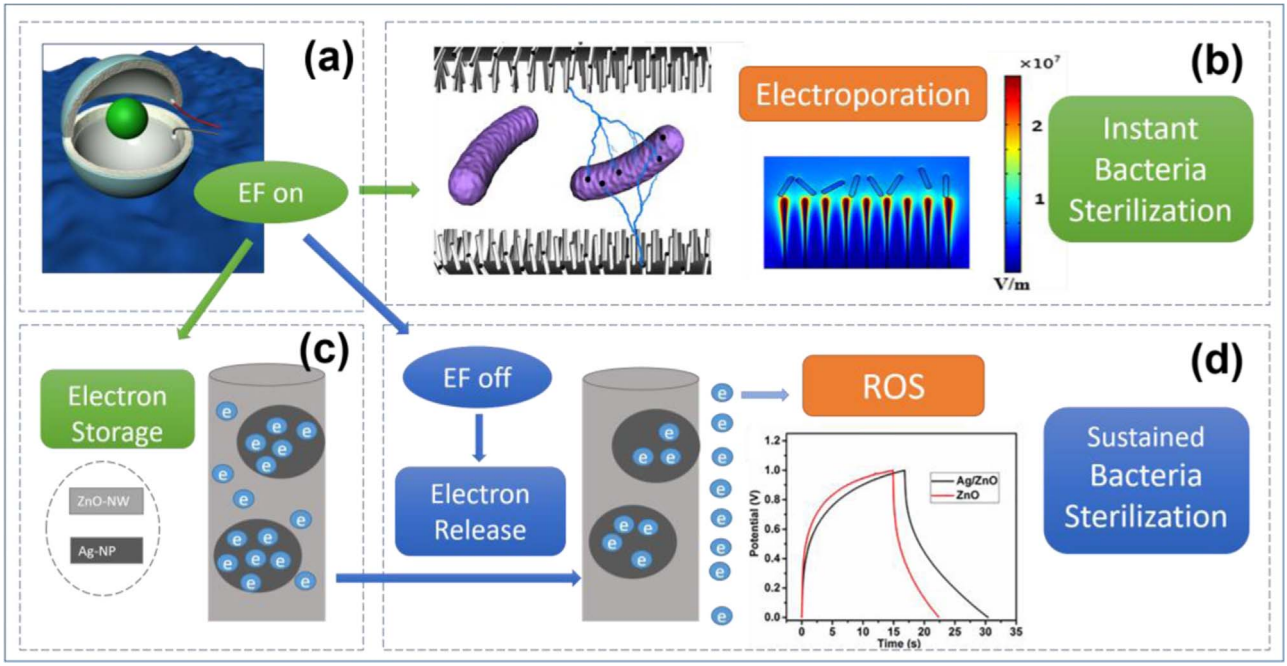

Fig. 5. Schematic figure of the synergetic mechanisms of the instant and sustained sterilization property of our system. (a) The wave driven TENG provide EF. (b) During EF supply, the Ag/ZnO nanobrush structure conducted electroporation in the bacteria cell. Simulation of EF intensity between the ZnO-NW tips and bacteria, showed that as high as 10^7 V/cm can be achieved near the surface of the nanowires. (c) During EF supply, electrons were stored in ZnO-NW, which would be released after EF was withdrawn, and continuously formed ROS for sustained bacteria sterilization. (d) When Ag-NP were integrated in ZnO-NW, the electron storage ability was greatly enhanced, so the more ROS were induced and much higher sterilization efficiency were achieved.

produced when the TENG was driven by waves produced by a periodic wave making machine (Jebao, WP-40, the power consumption 40 W) at about 2 Hz. The electricity could also be easily generated by simply hand shaking of the TENG. The electric characterizations were measured by Keithley 6517 System Electrometer and SR570 low noise current amplifier from Stanford Research Systems.

4.2. The growth of Ag/ZnO nanobrush on carbon cloth

ZnO-NW and Ag-NP were grown on CC [14,15], a woven textile material with good conductivity consisting of carbon fibers that were10 μm in diameter. The carbon cloth was cleaned with acetone and ethanol for three times, and then treated by oxygen plasma for 5 min before use. After Plasma treatment, the carbon cloth was treated with ZnO-NW seeds solution to initiate the ZnO-NW growth. Then ZnO-NW on the CC grew in aqueous solution by a wet-chemical method. After that, Ag-NP were loaded on ZnO-NW by a dip-in and light irradiation method. The detailed process was described in the Supporting information.

4.3. Bacterium cultivation

The sterilization efficiency was evaluated using two model bacteria and raw nature lake water. The model bacteria were bought from China Center of Industrial Culture Collection (CICC): *E. coli* (CICC23657) and *S. aureus* (CICC10384). They were cultured in LB (Luria-Bertani) medium at 37 °C for 18 h to the stationary phase after inoculation in a 120 rpm shakers. Then the bacteria solution was centrifuged at 6000 rpm, washed and resuspended in sterilizing physiological saline to reach a concentration of 1×10^6 CFU/mL. Moreover, the river water under Jimen Bridge in Beijing was collected to characterize the sterilization effect on natural water. The river water was driven by the pump to pass through the Ag/ZnO electrodes directly at the same parameters as the *E. coli* and *S. aureus* solutions, and the total CFU in the river water before and after the 25 min treatment were monitored.

4.4. Disinfection of the bacteria by the TENG and Ag/ZnO system

During sterilization operation, the electricity supplied by the TENG was applied to the Ag/ZnO nanobrush grown on the CC. The cloth were cut into circles with a size of φ=10 mm, and placed into two filter holders that were connected face to face as two electrodes. The bacteria solution passing through the filter were treated by the EF. The electricity generation lasted for only 5 min, then the TENG was stopped from working, while the sterilization efficiency was continuously tested in the following 20 min. Four experimental groups were tested: Ag/ZnO nanobrush with EF (Ag/ZnO+EF): Ag/ZnO nanobrush without EF (Ag/ZnO), ZnO nanobrush with EF (ZnO+EF), and original carbon cloth with EF (CC+EF). Bacteria solution passed through the electrical field dropwise at a constant rate of 1 mL/min driven by a peristaltic pump. Then they were collected, 10-fold serially diluted, plated on LB agar plate, and cultured at 37 °C for 18 h to do CFU counting. The time points were 0, 0.5, 2.5, 5, 10, 15, 20 and 25 min. The SR was calculated using the Equation

$$SR = \frac{CFU_0 - CFU_1}{CFU_0} \times 100\% \quad (3)$$

where CFU_0 is raw bacteria CFU/mL, CFU_1 is the bacteria CFU/mL after treatment.

4.5. Ion concentration measurement

Distilled water passing through the Ag/ZnO nanobrush was collected at 0.5, 2.5, 5, 10, 15, 20, 25 min for silver and zinc ions contents analysis, and the electricity supply stopped at 5 min. Inductively Coupled Plasma Optical Emission Spectrometer (ICP-OES, PerkinElmer, Optima 7000DV) was used to analyze the ions concentrations.

4.6. SEM observation

The bacteria morphology change was studied using SEM after fixation and dehydrations. First, the samples were fixed with 4% paraformalde-

hyde for 4 h, and then dehydrated in graded ethanol, 30%, 50%, 70%, 85% and 90% ethanol for 0.5 h each. After immersion in 100% ethanol for 0.5 h for 3 times, the sample was dried in air for 4 h under a fume hood. The samples were imaged using a field-emission scanning electron microscopy (FE-SEM, Hitachi SU8020) at a voltage of 5 kV.

4.7. Intracellular ROS monitoring

Four groups were monitored for their ability to induce intracellular ROS in the bacteria: Ag/ZnO nanobrush with EF (Ag/ZnO+EF), Ag/ZnO nanobrush without EF (Ag/ZnO), ZnO-NW with EF (ZnO+EF), ZnO-NW without EF (ZnO). At 0.5, 2.5, 5, 10, 20, and 25 min, the bacteria suspension were collected, centrifuged at 6000 rpm for 5 min, and stained with 10 μM 2′, 7′-dichlorodihydrofluorescein diacetate (DCFDA, Beyotime, China) at 37 °C for 15 min in darkness. Then they were rinsed with PBS, tested on flow cytometer (Accuri C6, BD) for FL-1 (530 nm) under 488 nm excitation light. For each sample, 10,000 bacteria were collected by the flow-cytometer and measured for their respective intracellular ROS signal intensity. An intensity threshold was set according to the control group, and was applied to all the treated groups. Thus the percentages of ROS signal positive cells could be compared among each group.

4.8. Electrical field simulation

The finite element method (FEM, COMSOL Multiphysics software) was used to calculate the electric field strength near the nanowires. The parameter were set as follows: Relative permittivity of water=81; Relative permittivity of ZnO=8.54; The Length of ZnO=3.5 μm; The Radius of ZnO=20 nm; The potential applied on the ZnO electrodes=50 V.

Acknowledgement

This work was supported by the national key R & D project from Minister of Science and Technology, China (2016YFA0202703), National Natural Science Foundation of China (NSFC 31571006, NSFC 81601629), Beijing Talents Fund (2015000021223ZK21) and "Thousands Talents" program for pioneer researcher and his innovation team. J.J. Tian, H.Q. Feng, and L. Yan contributed equally to this work.

Appendix A. Supplementary material

Supplementary data associated with this article can be found in the online version at doi:10.1016/j.nanoen.2017.04.030.

References

[1] M.A. Shannon, P.W. Bohn, M. Elimelech, J.G. Georgiadis, B.J. Marinas, A.M. Mayes, Nature 452 (2008) 301–310.
[2] M. Santosham, A. Chandran, S. Fitzwater, C. Fischer-Walker, A.H. Baqui, R. Black, Lancet 376 (2010) 63–67.
[3] S.D. Richardson, M.J. Plewa, E.D. Wagner, R. Schoeny, D.M. DeMarini, Mutat. Res.-Rev. Mutat. 636 (2007) 178–242.
[4] S.D. Richardson, TrAC-Trend Anal. Chem. 22 (2003) 666–684.
[5] B.E. Logan, M. Elimelech, Nature 488 (2012) 313–319.
[6] H. Zhou, D.W. Smith, Can. J. Civil. Eng. 28 (2001) 49–66.
[7] N.J. Rusell, M. Colley, R.K. Simpson, A.J. Trivett, R.I. Evans, Int. J. Food Microbiol. 55 (2000) 133–136.
[8] D. Knorr, M. Geulen, T. Grahl, W. Sitzmann, Trends Food Sci. Technol. 5 (1994) 71–75.
[9] T. Ohshima, K. Okuyama, M. Sato, J. Electrostat. 55 (2002) 227–235.
[10] S. Jayaram, G.S.P. Castle, A. Margaritis, Biotechnol. Bioeng. 40 (1992) 1412–1420.
[11] U. Zimmermann, Rev. Physiol. Biochem. Pharmacol. 105 (1986) 175–256.
[12] L. Gibot, M.P. Rols, Expert Opin. Biol. Ther. 16 (2016) 67–77.
[13] A. Grainys, V. Novickij, J. Novickij, Instrum. Sci. Technol. 44 (2016) 65–72.
[14] H.Y. Tang, T.J. Liu, P. Jiang, J. Nanosci. Nanotechnol. 13 (2013) 1385–1388.
[15] Z. Li, H.Y. Tang, W.W. Yuan, W. Song, Y.S. Niu, L. Yan, M. Yu, M. Dai, S.Y. Feng, M.H. Wang, T.J. Liu, P. Jiang, Y.B. Fan, Z.L. Wang, Nanotechnology 25 (2014) 145702.
[16] C. Liu, X. Xie, W. Zhao, N. Liu, P.A. Maraccini, L.M. Sassoubre, A.B. Boehm, Y. Cui, Nano Lett. 13 (2013) 4288–4293.
[17] Z.L. Wang, ACS Nano 7 (2013) 9533–9557.
[18] S. Kim, M.K. Gupta, K.Y. Lee, A. Sohn, T.Y. Kim, K.S. Shin, D. Kim, S.K. Kim, K.H. Lee, H.J. Shin, D.W. Kim, S.W. Kim, Adv. Mater. 26 (2014) 3918–3925.
[19] G. Zhu, Z.H. Lin, Q.S. Jing, P. Bai, C.F. Pan, Y. Yang, Y.S. Zhou, Z.L. Wang, Nano Lett. 13 (2013) 847–853.
[20] Y. Zheng, L. Cheng, M. Yuan, Z. Wang, L. Zhang, Y. Qin, T. Jing, Nanoscale 6 (2014) 7842–7846.
[21] B. Meng, W. Tang, X. Zhang, M. Han, W. Liu, H. Zhang, Nano Energy 2 (2013) 1101–1106.
[22] Q. Zheng, B.J. Shi, F.R. Fan, X.X. Wang, L. Yan, W.W. Yuan, S.H. Wang, H. Liu, Z. Li, Z.L. Wang, Adv. Mater. 26 (2014) 5851–5856.
[23] B.J. Shi, Q. Zheng, W. Jiang, L. Yan, X.X. Wang, H. Liu, Y. Yao, Z. Li, Z.L. Wang, Adv. Mater. 28 (2016) 846–852.
[24] W. Tang, J.J. Tian, Q. Zheng, L. Yan, J.X. Wang, Z. Li, Z.L. Wang, ACS Nano 9 (2015) 7867–7873.
[25] Q. Zheng, Y. Zou, Y.L. Zhang, Z. Liu, B.J. Shi, X.X. Wang, Y.M. Jin, H. Ouyang, Z. Li, Z.L. Wang, Science Advances 2 (2016) e1501478.
[26] X.F. Wang, S.M. Niu, Y.J. Yin, F. Yi, Z. You, Z.L. Wang, Adv. Energy Mater. 5 (2015) 1501467.
[27] J. Chen, J. Yang, Z.L. Li, X. Fan, Y.L. Zi, Q.S. Jing, H.Y. Guo, Z. Wen, K.C. Pradel, S.M. Niu, Z.L. Wang, ACS Nano 9 (2015) 3324–3331.
[28] Y. Yang, H.L. Zhang, R.Y. Liu, X.N. Wen, T.C. Hou, Z.L. Wang, Adv. Energy Mater. 3 (2013) 1563–1568.
[29] L.M. Zhang, C.B. Han, T. Jiang, T. Zhou, X.H. Li, C. Zhang, Z.L. Wang, Nano Energy 22 (2016) 87–94.
[30] T. Jiang, L.M. Zhang, X.Y. Chen, C.B. Han, W. Tang, C. Zhang, L. Xu, Z.L. Wang, ACS Nano 9 (2015) 12562–12572.
[31] Z.H. Lin, G. Cheng, W.Z. Wu, K.C. Pradel, Z.L. Wang, ACS Nano 8 (2014) 6440–6448.
[32] L. Xu, Y. Pang, C. Zhang, T. Jiang, X. Chen, J. Luo, W. Tang, X. Cao, Z.L. Wang, Nano Energy 31 (2017) 351–358.
[33] M.A. Maurer-Jones, M.P.S. Mousavi, L.D. Chen, P. Buhlmann, C.L. Haynes, Chem. Sci. 4 (2013) 2564–2572.
[34] B.D. Shepard, M.S. Gilmore, Methods Mol. Biol. 47 (1995) 217–226.
[35] G. Gogniat, S. Dukan, Appl. Environ. Microbiol. 73 (2007) 7740–7743.
[36] E. Cabiscol, J. Tamarit, J. Ros, Int. Microbiol. 1 (2000) 3–8.
[37] O. Blokhina, E. Virolainen, K.V. Fagerstedt, Ann. Bot.-Lond. 91 (2003) 179–194 (Spec No. 2).
[38] M. Haase, H. Weller, A. Henglein, J. Phys. Chem.-US 92 (1988) 482–487.
[39] Z.L. Wang, R. Guo, G.R. Li, L.X. Ding, Y.N. Ou, Y.X. Tong, RSC Adv. 1 (2011) 48–51.
[40] T. Hirakawa, P.V. Kamat, Langmuir 20 (2004) 5645–5647.
[41] H.L. Cao, Y.Q. Qiao, X.Y. Liu, T. Lu, T. Cui, F.H. Meng, P.K. Chu, Acta Biomater. 9 (2013) 5100–5110.
[42] S.R. Morrison, T. Freund, J. Chem. Phys. 47 (1967) 1543–1551.
[43] C. Liu, X. Xie, W. Zhao, J. Yao, D. Kong, A.B. Boehm, Y. Cui, Nano Lett. 14 (2014) 5603–5608.
[44] E.L. da Silva, M.K. Piskula, N. Yamamoto, J.H. Moon, J. Terao, FEBS Lett. 430 (1998) 405–408.
[45] S. Clemens, M.G. Palmgren, U. Kramer, Trends Plant. Sci. 7 (2002) 309–315.
[46] L. Savarino, D. Granchi, G. Ciapetti, E. Cenni, G. Ravaglia, P. Forti, F. Maioli, R. Mattioli, Exp. Gerontol. 36 (2001) 327–339.
[47] N.J. Hare, N.E. Scott, E.H.H. Shin, A.M. Connolly, M.R. Larsen, G. Palmisano, S.J. Cordwell, Proteomics 11 (2011) 3056–3069.
[48] H.Q. Feng, R.X. Wang, P. Sun, H.Y. Wu, Q. Liu, J. Fang, W.D. Zhu, F.T. Li, J. Zhang, Appl. Phys. Lett. 97 (2010) 131501.
[49] D.J. Dwyer, P.A. Belenky, J.H. Yang, I.C. MacDonald, J.D. Martell, N. Takahashi, C.T.Y. Chan, M.A. Lobritz, D. Braff, E.G. Schwarz, J.D. Ye, M. Pati, M. Vercruysse, P.S. Ralifo, K.R. Allison, A.S. Khalil, A.Y. Ting, G.C. Walker, J.J. Collins, Proc. Natl. Acad. Sci. USA 111 (2014) E2100–E2109.
[50] N. von Moos, V.I. Slaveykova, Nanotoxicology 8 (2014) 605–630.
[51] R.N. Ma, H.Q. Feng, J.S. Guo, Y.D. Liang, Q. Zhang, Y. Tian, J. Zhang, J. Fang, Plasma Process Polym. 11 (2014) 822–832.
[52] J.J. Foti, B. Devadoss, J.A. Winkler, J.J. Collins, G.C. Walker, Science 336 (2012) 315–319.
[53] C. Nathan, A. Cunningham-Bussel, Nat. Rev. Immunol. 13 (2013) 349–361.
[54] M. Okamura, M. Paddock, M. Graige, G. Feher, Biochim. Biophys. Acta (BBA)-Bioenerg. 1458 (2000) 148–163.
[55] J.F. Turrens, Reactive Oxygen Species, Encyclopedia of Biophysics, Springer, 2013, pp. 2198–2200.
[56] G. Wang, W. Jin, A.M. Qasim, A. Gao, X. Peng, W. Li, H. Feng, P.K. Chu, Biomaterials 124 (2017) 25–34.
[57] H.L. Zhang, Y. Yang, Y.J. Su, J. Chen, K. Adams, S. Lee, C.G. Hu, Z.L. Wang, Adv. Funct. Mater. 24 (2014) 1401–1407.

Jingjing Tian received the B.E degree in Yantai University, China, in 2013. She is currently pursuing the Ph.D. degree at Beijing Institute of Nanoenergy and Nanosystem, Chinese Academy of Sciences. Her research work is focusing on the application of nanogenerator on antibacterial and self-powered biomedical system.

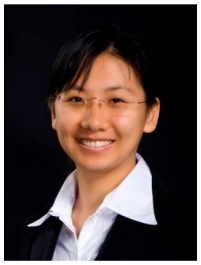

Dr. Hongqing Feng received her Bachelor's Degree and Doctor's Degree in Peking University, Beijing, China. She is currently working as the assistant professor at Beijing Institute of Nanoenergy and Nanosystems, Chinese Academy of Science. Her research interest includes antibacterial technologies and implantable nanogenerators.

Ling Yan received the B.E. degree in Bioengineering from Beihang University, Beijing, China, in 2013. And received the M.A. degree in School of Biological Science and Medical Engineering, BUAA, Beijing, China, in 2016. His research interests is focusing on the antibacterial nano-materials.

Dr. Min Yu received her Ph.D. degree from Peking University in department of Biomedical Engineering in 2010, and M.D. from Medical School of Wuhan University in 2004. Currently, she is a visiting research assistant in Beijing Institute of Nanoenergy and Nanosystems.

Han Ouyang received the B.S. degree in Material Physics from southwest university of science and technology, China, in 2014. He is current pursuing the Ph.D. degree at Beijing Institute of Nanoenergy and Nanosystems, Chinese Academy of Sciences. His research work is focusing on self-powered sensor systems.

Hu Li received the B.S. degree in School of Material Science and Engineering from Tianjin Polytechnic University, Tianjin, China, in 2014. He is currently pursuing the Ph.D. degree in School of Biological Science and Medical Engineering, Beihang University, Beijing, China. His research work is focusing on nanogenerator, active sensors, energy storage device and self-assembly of nanomaterials.

Dr. Wen Jiang received his Ph.D. degree from National Center for Nanoscience and Technology, China, in 2017, and master degree from Qingdao Institute of Bioenergy and Bioprocess Technology, Chinese Academy of Sciences. His research interests include nanogenerator and implantable self-powered biomedical devices.

Yiming Jin received the B.S. degree in Qingdao University of Science and Technology, China. He received the M.E. degree in Beijing Institute of Nanoenergy and Nanosystems, Chinese Academy of Sciences in 2016. He is currently pursuing his Ph.D. degree at Helmholtz-Zentrum, Germany. His research focus is nanogenerator and its application in biological signal sensing.

Dr. Guang Zhu is a professor at Beijing Institute of Nanoenergy and Nanosystems, Chinese Academy of Sciences. He received his Ph.D. degree in Materials Science and Engineering at Georgia Tech in 2013 and his Bachelor degree in Materials Science and Engineering at Beijing University of Chemical Technology in 2008. His current research mainly focuses on designing, fabrication, and implementation of innovative miniaturized high-efficiency generators that harvest and convert ambient mechanical energy into electricity.

Prof. Zhou Li received his Ph.D. from Peking University in Department of Biomedical Engineering in 2010, and bachelor degree from Wuhan University in 2004. He jointed School of Biological Science and Medical Engineering of Beihang University in 2010 as an associate Professor. Currently, he is a Professor in Beijing Institute of Nanoenergy and Nanosystems, CAS. His research interests include nanogenerators, *in vivo* energy harvester and self-powered medical devices, biosensors.

Dr. Zhong Lin Wang is a Hightower Chair and Regents's Professor at Georgia Tech. He is also the Chief scientist and Director for the Beijing Institute of Nanoenergy and Nanosystems, Chinese Academy of Sciences. His discovery and breakthroughs in developing nanogenerators establish the technological roadmap for harvesting mechanical energy from environmental and biological systems for powering personal electronics. He pioneered the field of piezotronics and piezo-phototronics by introducing piezoelectric potential gated charge transport process in fabricating new electronic and optoelectronic devices. This historical breakthrough by redesigning CMOS transistor has important applications in smart MEMS/NEMS, nanorobotics, human-electronics interface and sensors.